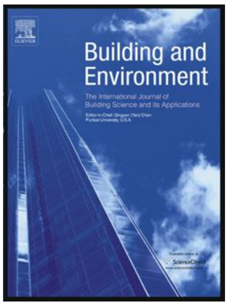

Assessment of wind-driven rain impact, related surface erosion and surface strength reduction of historic building materials

Aykut Erkal, Dina D'Ayala, Lourenço Sequeira

PII: S0360-1323(12)00152-7

DOI: 10.1016/j.buildenv.2012.05.004

Reference: BAE 3157

To appear in: *Building and Environment*

Received Date: 2 January 2012

Revised Date: 11 May 2012

Accepted Date: 14 May 2012

# Assessment of Wind-driven Rain Impact, Related Surface Erosion and Surface Strength Reduction of Historic Building Materials

Dr. Aykut Erkal [a], Dr. Dina D'Ayala [b], Mr. Lourenço Sequeira [c]

[a] Corresponding Author, Research Officer, Department of Architecture and Civil Engineering, 6 East 3.14, University of Bath, BA2 7AY, Bath, UK.
Phone: +44 1225 386749; Mobile: +44 7586 470044; Fax: +44 1225 386691
Email: erkala@hotmail.com

[b] Reader, Department of Architecture and Civil Engineering, 6 East 4.8
University of Bath, BA2 7AY, Bath, UK.
Phone: +44 1225 386749; Mobile: +44 7754185807; Fax: +44 1225 386691
Email: absdfda@bath.ac.uk

[c] Student, Department of Architecture and Civil Engineering,
University of Bath, BA2 7AY, Bath, UK.
Mobile: +44 7878 749577; Fax: +44 1225 386691
Email: lourenco89@hotmail.com

**Abstract**

Building surface erosion is a common phenomenon observed on historic building façades due to wind-driven rain (WDR) impact. Recently, studies on climate change and the effect this might have on increased extreme rainfall events has renewed the scientific interest on determining the risk of accelerated erosive effects. Given the fact that WDR loads on building façades is proportional to rainfall and represents the main moisture source and erosive physical impact for building façades, an assessment method that quantifies the severity of erosion is the first step towards recommending remedial measures. The paper discusses the major factors escalating the gradual loss of surface material, considering value, hazard, vulnerability and exposure in order to examine the WDR drop impact on the aesthetic significance and the structural integrity of heritage buildings, within a parametric framework. The study investigates the effects of different size water drops, with different impact speeds on a range of masonry materials with different surface asperities and varying moisture absorption features, at various impact angles. For the relative quantification of the long-term surface erosion, straightforward and globally adaptable experiments are proposed based on site-specific climatic data and materials. Finally, strength decline of exposed sample units proves the strength-degrading effect of erosive WDR.

**Keywords**: Façade erosion; Raindrop impact; Wind-driven rain; Building conservation; Historic Buildings; Building sustainability.

## 1. Introduction: Objectives, State-of-the-art and Methodology

Widespread major weather events all over the world have focussed attention on the influential effects of climate change. In June 2007, in excess of 150 mm of rain fell over much of Wales, the Midlands, Northern England, Northern Ireland and parts of Scotland and South-west England. [1]. Other notable examples include the floods in central Europe in 2002, the New Orleans flood in 2005 and numerous floods in South Asia in 2007 and 2009 [2]. Heavy rain fall, flooding and strong winds or storms have had severe impact on the social, economic and cultural spheres of the country life. Although the consequences of these extreme weather events have been investigated in various sectors (i.e. agriculture, industry, energy, transport), damaging effects on the cultural heritage have insufficiently been addressed [3]. The changing magnitude of extreme weather events has

ACCEPTED MANUSCRIPT

emphasised the need to review the damaging factors in surface deterioration (Fig 1) and eventually loss of integrity of heritage buildings to identify, quantify, and control the climatic effects for evaluation of remedial strategies.

The study presents novel objectives: (i) Firstly, to define a robust risk assessment framework within which the major factors escalating the loss of surface erosion are documented and classified according to value, hazard, vulnerability and exposure. (ii) Secondly, to identify the dominant factors and their implication on the aesthetic significance and structural integrity of heritage buildings. Impact behaviour examination of varying size water drops with varying speeds and impacting angles forms the parametric framework, wherein a range of masonry materials with different surface asperities and moisture absorption features, are being comparatively tested. (iii) Thirdly, a straightforward and adaptable testing regime to quantify the surface erosion due to long-term WDR impact is proposed, relating the drop impact size and duration to the local rainfall characteristics. (iv) Lastly, the study aims to measure the strength decline of exposed sample units after erosive WDR effect using a modestly destructive technique that can be used on site.

## 2. Evidence of Wind-driven Rain Erosion on Historic Masonry Building Façades

Several researchers emphasised the adverse effects of WDR on various building materials. For instance, rain has been noted to be an important contributory factor to the extent of stone erosion [4]. Importantly, clean rain is considered the cause for surface erosion of building façades [5]. For instance, the effect of WDR on surface stone erosion has been investigated at the Cathedral of Learning, a tall limestone building in Pittsburgh, Pennsylvania [6, 7]. Numerical modelling and field measurements of WDR loads on the façades showed that white, eroded areas on the building's walls corresponded to sections receiving high amounts of WDR fluxes. For the same building, Etyemezian et. al. [8] also reported that the calculated rain fluxes on the façade of the building were reasonably consistent with the erosion patterns. Monumental brick masonry is also susceptible to WDR erosion as reported for St Hubertus, in the Netherlands, where climatic conditions are similar to the UK. Numerical simulation and on-site WDR measurements were performed to determine the amount of WDR on the most damaged south-west façade [9]. Surface deterioration of granite buildings in Aberdeen, Scotland, is also noteworthy. On the highly exposed façades of some of the buildings, WDR caused mortar erosion and dampness problems and re-pointing was performed as a remedial measure for the façade [10]. Dramatically, for earth-wall buildings, the impact becomes more critical. Heathcote [11] reported that the release of the kinetic energy associated with raindrops impacting on the building façade is the main cause for the removal of material from the surfaces. Furthermore, abrasive action of raindrops on cement stabilised rammed earth wall surfaces is also evident and stabilising the soil with a chemical agent such as cement was noted to eliminate, to some extent, this drawback [12]. Similarly, in a study performed with compressed and cement-stabilised building blocks by Kerali (2001), the conclusion was surface erosion due to WDR varies according to the elevation of the block within the wall, orientation of the façade, and the age of the building (period of exposure) [13].

## 3. Factors Affecting Façade Erosion due to Raindrop Impact

Rain with a horizontal velocity component given by the wind is called wind-driven rain (WDR) [14], which is one of the main factors being responsible for surface erosion. Erosion here means the material detachment from a masonry building façade due to the physical impingement effect of WDR. Detachment occurs through long-term, continuous, repetitive and synergetic action of WDR. The loss of surface material can be quantified by a probabilistic approach to enable variation and uncertainty, and defined as a probability function of value, hazard, vulnerability and exposure. This can be applied to a single feature on a façade (an ornament), a complete façade, a whole building or the historic building stock in a historic centre. The major contributing factors can be expressed with regard to the respective components:

$$P_{\text{Surface Erosion}}(\text{Loss}) = P(\text{Value}) \cdot P(\text{Hazard}) \cdot P(\text{Vulnerability}) \cdot P(\text{Exposure}) \quad (1)$$

Equation (1) provides a probabilistic-based qualitative understanding of the predominant and independent variables determining surface erosion. Similar approach has also been used to evaluate other natural disastrous effects by other researchers [15]. This formulation can be best understood by examining different locations on the façades of the southern transept of Tewkesbury Abbey (Fig.1). For instance, very heavy rainfalls (high hazard) on the south east façade (high exposure) causes high physical loss (as the material is vulnerable, see loosening of the masonry) but modest overall loss as there is no ornament (low value) (Fig.1a). Similarly, heavy rainfalls (high hazard) will not cause loss to a well-protected (shielded) façade (low exposure) although the material might be just as vulnerable and has greater value (Fig.1b). However, even moderate rain events (medium hazard) will result in relatively more erosion to the moulded unprotected façade (high exposure, high value, and high vulnerability) (Fig.1c). Besides material type (vulnerability) and façade orientation with respect to prevailing wind direction (directional exposure) (Fig.1a and Fig.1c), an important factor is also the duration of any event determining the time exposure. Each variable will now be discussed in-detail.

### 3.1. Value

By value is intended the appreciation (cultural, social, historical) of the fabric of a historic building due to its authenticity and the added value of human interaction with the material (Fig. 1). When there is no substance to erode, there is neither risk nor loss. However, most cultural heritage presents delicate ornamentation and exquisite craftsmanship having historical and evidential importance. Protection of cultural identity from the threat of accelerating climatic events becomes necessary. The protection of Sueno's Stone, a sculptured sandstone monument dating from the end of the first millennium AD on the north-easterly edge of Forres, Scotland well clarifies the concept [16]. The monument was covered by protective glass to explicitly prevent further deterioration of the carved sandstone from WDR and wind erosion. In an even more extreme intervention, the original statues of the west front of Wells Cathedral have been replicated and removed to avoid further loss of material and value [17].

### 3.2. Hazard

Hazard is the erosive effect of impinging raindrops. Paramount factor for its quantification is WDR loads delivered to the wall surfaces. As an easily measurable parameter, the total rainfall is a reliable indicator of the relative WDR loads. For instance Tang et. al., (2004) measured WDR loads on a building at 16 locations together with rainfall data [6]. The conclusion was that total WDR loads on building façades for each storm are increasing with the increase in rainfall.

Importantly, processes of naturally occurring surface erosion are expected to be accelerated by the changes in weather patterns observed by [1], [18] and [19]. For instance, analyses of historical weather records show that all regions of the UK have experienced an increase over the past 45 years in the contribution to winter rainfall from heavy precipitation events. Severe windstorms around the UK have become more frequent in the past few decades [20]. More importantly, projections indicate that changes in mean precipitation for the 2080s under the medium emissions scenario demonstrate that in winter, precipitation increases are in the range +10 to +30% over the majority of the country. The biggest changes (those at the 50% probability level) in precipitation in winter, increases up to +33%, are seen along the western side of the UK [18]. The data from Meteorological Office [1] depicted in Fig. 2 shows seasonal rainfall trends between 1910 and 2010 where increased rainfall is observed over springs and autumns. The implication from a seasonal point of view is that, the building façades are subjected to WDR longer and the moisture can penetrate deep into the walls causing potential stone decay as indicated by Smith et.al. [19].

To quantify WDR loads, there are three approaches: (i), semi empirical (ii) experimental and (iii) numerical analysis [14]. Due to simplicity of application, semi-empirical WDR relationships have been a widely used method, employing standard weather data (wind speed, wind direction and horizontal rainfall). Primarily, a frequently used relationship to predict WDR loads $R_{wdr}$ on buildings is [21, 22]:

$$R_{wdr} = \alpha \cdot U \cdot R_h^{\ 0.88} \cdot \cos\beta \qquad (2)$$

where $\alpha$ is the adapted WDR coefficient (s/m) which takes into consideration the site topography and the presence of building itself. In many studies, $\alpha$ has taken various values between 0.02 s/m and 0.26s/m depending on the building size and location on the façade [22]. $U$ is the reference wind speed measured at the standard meteorological height of 10m (m/s), $R_h$ is the unobstructed rainfall intensity and $\beta$ is the wind incidence angle between wind direction and the normal to the wall surface, requiring that component of the wind velocity normal to the wall surface is taken [14]. Critically, Equation (2) constitutes the basis for the latest ISO 15927-3:2009 for calculation of WDR [23].

**3.3. Vulnerability**

Lack of resistance to surface erosion constitutes the vulnerability component. Historic building wall substance and surface properties are critical. Each building material generally has a characteristic range of particle bond strength [13]. The weaker the bond is, the easier the material detachment is to occur, disrupting the bond among the constituent particles. Porosity and tortuosity is another factor in terms of rendering inner layers more vulnerable to atmospheric effects. Equally important, the likelihood of particle disturbance on a rough wall surface induced by rain impingement is higher than on a wall of the same material with smoother surface due to the reduced frictional forces [11]. Additionally, wall construction systems comprising different materials with different construction techniques can be critical since different erosion rates of different materials could cause more complicated surface and interface degradation.

**3.4. Exposure**

"Exposure" account for (i) ambient conditions of the building and (ii) the effect of time. Façade orientation with respect to the direction of the prevailing winds is crucial because prevailing winds drive the rain on the exposed façades. Even different locations over the façade are decisive parameters for the magnitude of surface degradation. Another factor is the extent of overhanging eaves, protecting wall surfaces. Also, adjacent disturbances such as trees and neighbouring buildings could provide variable shielding against wind and rain.

Time is dominant as erosion occurs over a very long time (i.e. years). Exposure can be defined as the time span considered determining perceptible erosion. Within this time frame, it is possible to determine the joint occurrence of rain and wind, blowing in a specific direction against a wall. To reflect this, Equation 2 can be integrated over the time span to calculate the total WDR load at a specific location on the wall, taking into account the windward rain events for a particular façade orientation.

## 4. Parametric Raindrop Impact Behaviour Testing

### 4.1. Drop Impact

Drop impact on solid and liquid surfaces has been studied by many researchers as the phenomenon has been the central issue in many applications [24]. Studies have not only concentrated on the drop impact on liquids [25], but also placed emphasis on solid and dry surfaces, experimentally investigating the relevance of impacting factors with high resolution digital photography [26] and to theoretically develop quantitative models [27]. Efforts were even extended on different specific types of materials such as wood with different density, surface properties and water absorbability [28] or on aluminium and glass plate surfaces [29]. Three-dimensional finite element modelling was also performed to determine the response of deformable surfaces due to arbitrary water drop collisions [30]. However, porous building materials have interestingly been studied far less [31,32, 33]. The main reason for this was probably the challenge of the extremely complicated flow patterns caused by the surface texture influence. Work by Rioboo et. al. supports this since they reported six possible drop impact behaviour for dry surfaces: deposition, prompt splash, corona splash, receding break-up, partial rebound and complete rebound [34]. Abuku et. al. (2009) performed the first measurements of the oblique drop impact of on a smooth ceramic brick surface, with drop diameters of 2 mm and 3.9 mm [35]. However, oblique drop impact has never been investigated on different porous masonry materials with a wider range of drop size, in a comparative fashion. This study aims to fill this gap.

### 4.2. Testing Parameters, Considerations and Methodology

To understand the response of the different masonry materials to WDR impact, solid hand-cut historic clay bricks (19th century), fired clay bricks (Berkeley Red Multi), unfired clay bricks (Ecoterre), and lime mortar were selected in the structures laboratory of the University of Bath. The test is designed to simulate variability of hazard by employing a range of water drops with a range of impact speeds under varying exposure condition by changing the specimen orientation and for different vulnerability condition by considering different masonry materials. There are three aims: (i) The main aim is to observe the role of different masonry materials impacted by water drops of varying diameters, impact speeds and impact angles. This will help to form an opinion about how the energy of the water drops tends to release on the surface with respect to related behaviour. Because the raindrops are assumed to be pure liquid water, viscosity and surface tension of a raindrop are considered constant and thus inconsequential for this study [35]. (ii) The second aim is to see how much water is held by the specimen surface after the water drop impingement depending on masonry material type. During a rain event, not all of the raindrops stick to the wall surface and therefore not all of them present a source of moisture for the wall; a portion of some of the raindrops can move away after the drops hit the surface (bouncing or splashing). WDR gauges collect all of the raindrops therefore the amount of WDR collected in WDR gauges can be different from the amount which actually acts as a moisture source. Differences bear importance for numerical analyses. (iii) The third aim is to have an idea about the role of different surface roughness and absorption features on the impact behaviour.

Drop diameters of 1.95 mm, 3.07 mm, and 4.06 mm were considered suitable and reasonably conservative for the testing, contributing largely to the erosive energy and being also used in other similar raindrop impact studies [35]. Importantly, existing literature on the field studies of raindrop size distribution reveals that the maximum drop size selected for the testing is not negligible considering an extreme and erosive rain event [36, 37, 38, 39]. Additionally, Best's raindrop size distribution model [40] which was established based on the rainfalls in USA, Canada and UK confirms that heavy rain events having more than 10mm/hr rainfall intensity present reasonable portion of raindrops with 4mm diameter [41]. Selected drops were released at heights of 2.10 m, 3.20 m, and 4.00 m respectively through a hypodermic needle and burettes on four different types of masonry materials. To see the effect of impact angle, the masonry specimens were placed on a table with inclined surfaces at five different angles of 5º, 15º, 25º, 35º, and 45º from the vertical to simulate the fact that specific wind flow patterns developed around buildings can drive rain drops onto wall surface at varied angles. The maximum release of kinetic energy occurs at an angle of 90° (perpendicular to the wall). However, potential removal of particles can more easily be initiated by a smaller angle owing to its prising effect. Therefore, acute impact angles considered, allows incorporating both of kinetic energy release and drop prising effect to initiate the disintegration. The angles were adjusted with a digital angle finder. Fig. 3 illustrates the testing setup. To capture the behaviour and determine the impact speed, a high speed camera (Photron - FASTCAM-X 1280PCI 4K) was used. A frame rate of 2000 frames per second was used for all of the tests. A resolution of 320 x 256 pixels was used as it was sufficient to capture the behaviour of the drops. Table 1 illustrates the testing parameters with respect to the tests on four different masonry materials, at five different angles. Fig. 4 shows a the stain from a digital camera and still frames from the high speed camera of the bouncing behaviour after some run-off of a 4.06mm diameter droplet from a height of 4.0 m on the solid hand-cut historic clay brick at 5°.

For each drop impact, 2 specimens of the same material were used and the experiments of drop impact were conducted twice to ensure repeatability. Material selection is based on bond strength, surface roughness, unit age, and material type or function. Unfired clay bricks (Ecoterre) are quite weak with respect to their bond strength [42]. Fired clay bricks (Berkeley Red Multi) have a relatively rough surface. Solid hand-cut historic clay bricks are from the Victorian period. Finally, lime mortar is one of the most common binders in historic buildings. The air lime mortar used was the one found attached to the hand-cut bricks reclaimed from a 19$^{th}$ Century building, and hence also historic.

Although the drop behaviour is complicated to describe exactly, to evaluate the drop impact results, the dominant drop behaviour as adhesion, splashing, bouncing, or run-off, occurring in a few milliseconds, was considered appropriate, when influential parameters for building materials such as surface wettability, roughness, position and porosity of masonry materials are taken into account [43]. The width and the length of the drop stains on each unit were measured with a calliper and recorded. A stain aspect ratio (SAR) is defined as the ratio of drop stain width to drop stain length on material surface after impingement. SARs are plotted for each test, for each material and impact angle (Fig. 5). Sample drop stains are shown in Fig. 6 through which SAR value of each drop is calculated.

**4.3. Surface Roughness Determination of Masonry Materials**

Effects of solid material surface topography on the drop impact phenomenon have widely been investigated. Commonly, surface topography can be classified into two groups. (i) On patterned solid surface textures, either a liquid drop fills the cavities of the surface texture (collapsed state) [44] or entrap the surrounding gas inside the surface cavities (suspended state) [45]. (ii) On the surfaces with randomly shaped asperities, characterisation of the impact becomes more difficult where the surfaces are characterized by a mean surface roughness parameter. Historic masonry material surfaces generally falls in this group and roughness plays a crucial role on the outcomes of drop impact phenomenon [26, 46, 47]. For example, Rioboo et al. experimentally studied the impact of drops onto solid dry surfaces and concluded that, roughness has an instant effect on the possibility of prompt splash behaviour [26]. They also added that the excessive number of influencing factors such as impact velocity, drop diameter, liquid viscosity, surface tension, surface wettability, wavelength and roughness generally preclude any universal correlation with any impact behaviour. If the surfaces are highly complex, having textured or porous surfaces or non-uniform surface wettability features, the characterization of the impact becomes much more challenging [48]. Various outcomes can be observed for drop impact onto rough and porous substrates whose understanding is significantly more complex than drop impacts onto simple surfaces [47]. If the impact is on the inclined surfaces as in the case of WDR rain impingement, a parametric study with varying impact angles can best investigates the phenomenon.

Herein, four different surface roughness features of the chosen porous masonry materials representing relative vulnerability levels facilitate the comparison of the drop impact. A laser scanner (PROSCAN 2000) with an accuracy of 1 μm (micrometre) while being limited to a surface roughness depth of 5mm was used for the determination of the surface roughness of the materials (Fig. 7). During the preliminary measurements, the laser scanner was configured to scan the surface in steps of 20 μm for each step, with 500 steps in the x and y directions to give a scanned area of 10 mm by 10 mm. This configuration was considered as a good compromise between the holistic surface roughness at a spot and the measurement time. It was decided to measure the surface roughness of each masonry material at five different locations and take the average of these roughness measurement values. The grooves on the unfired clay bricks (Ecoterre) have a curved profile and the laser scanning analysis software could not alter the data properly to take the curve into account. Thus, only the data measured in the y direction was taken into account because the grooves have a fairly consistent elevation in the y direction.

The roughness values ($R_a$) acquired for the x and y directions for each material and displayed in Table 2 are the arithmetic average deviations of the assessed profile [49], as calculated by the laser scanner analysis software by taking the arithmetic average of the absolute values of the roughness profile ordinates $|Z(x)|$ all over the entire sampling length $l$ using Equation (3). The roughness profile for solid hand-cut historic clay brick in Test 4 is displayed in Fig. 7.

$$R_a = 1/l \int_0^l |Z(x)| \, dx \qquad (3)$$

### 4.4. Water Absorption Characteristics of Masonry Materials

The absorption characteristics of masonry materials having fine-pored surfaces are identified as essential parameters since they govern the immediate impact behaviour, penetration of impacting water drops and retention of moisture. For instance, a material with a high absorption rate will absorb and retain more water from WDR than a material with a low absorption rate [35] or impact behaviour would result in different outcomes such as drop stain lengths and widths [31, 48]. Therefore, the tests to determine the “Initial rate of water absorption of clay masonry units” is regarded as appropriate and performed in accordance with BS EN 772-11:2000 [50] where the principle is to dry the material to a constant mass, immerse the relevant face of the material in water for a period of time (60 seconds) and determine the increase in mass according to Equation (4).

$$c_{wi,s} = \left[\left(m_{so,s} - m_{dry,s}\right)/A_s\, t\right] \times 10^3 \;\; \left[kg/\left(m^2 \times \min\right)\right] \qquad (4)$$

where $m_{dry,s}$ is the mass of the specimen after drying, (g); $m_{so,s}$ is the mass of the specimen after soaking for time *t*, (g); $A_s$ is the gross area of the face of the specimen immersed in water, (mm$^2$); t is the time in minutes, set as 1 minute for this test. Only one face of the unit is in contact with water while the others are in contact with air. The test provides an understanding of one-dimensional water absorption into a semi-infinite medium. The flow is normal to the inflow face throughout the wetted face to which the equipotentials are parallel [51]. Fig. 8 shows the testing of solid hand-cut historic clay bricks. The unfired clay bricks (Ecoterre) had to be omitted from absorption tests as they disintegrate when immersed in water.

To simulate the processes occurring when clay masonry units are subjected to large amounts of WDR impact for longer period of time, the water absorption test was performed in accordance with BS EN 771-1:2003 (Annex C) [52] as this takes into account better the effects of micro-structural features such as amount, size and shape of pores because this standard requires greater contact to water for longer time. Oven-dried samples having dry mass, $m_d$ were placed in a tank of water for 24 hours (all faces of the units were kept in contact with water), after which the wet mass of each unit was determined, $m_w$. The water absorption $w_m$ is calculated according to Equation (5).

$$w_m = [(m_w - m_d)/m_d] \times 100 \ [\%] \tag{5}$$

The initial rate of water absorption ($c_{wi,s}$) and water absorption ($w_m$) test results for each masonry material are displayed in Table 3. Increasing water absorption rate represents increasing vulnerability to WDR.

## 5. Surface Erosion Testing

To make practical surface erosion predictions, a straightforward and globally adaptable testing method has been presented. Although similar tests have previously been conducted, they were only used to determine the suitability of soil to be used in adobe structures (whether there is a need for stabilisation) based on pitting depth due to the effect of water drops or water jet [53]. Therefore, parameters, considerations and methodology are discussed for a relative assessment of surface erosion and strength degradation.

### 5.1. Testing Parameters, Considerations and Methodology

Three solid hand-cut historic clay bricks due to their historic nature and relatively high $c_{wi,s}$ and $w_m$ values and three unfired clay bricks (Ecoterre) due to their low bond strength were tested in Erosion Test 1 and in Erosion Test 2, respectively to quantify surface erosion and moisture retention. Vulnerable regional materials can be identified in different areas with a similar fashion. Burettes were used with and without plastic nozzles attached to their tips to produce 3.07mm and 4.06mm diameter drops, respectively, knowing their high contribution to the erosive kinetic energy [54]. The burettes were placed at a height of 4.0 m above the intended points of impact on the masonry units and supported by clamps. The water amount to impact on the surface of units was calculated based on the climatic data from Boscombe Down and Lyneham between 1971 and 2000. Fig. 9 shows monthly rainfall and wind speed averages through a year. Maximum representative WDR amounts can be quantified for the erosion tests utilizing Equation (2). The main reasons for the selection of these locations are the proximity of the places to major historic city centres such as Tewkesbury and Winchester in the south-west of the UK and the ease of the accessibility and availability of the climatic data. It is noted from Fig. 9 that in the winter and autumn months, wind speed averages increase with the increasing rainfall.

Rain intensity vectors have been determined as a resultant vector of wind speed and falling drop terminal velocity for each drop size (Fig. 10). For the horizontal component of rain intensity vector, an average wind speed value of 4.5m/s for Boscombe Down and Lyneham has been used based on available monthly average data between 1971 and 2000 (Fig. 9). Impact velocities of drops falling from 4.0m height and impact angles based on rain intensity vectors were estimated as 7.4m/s and 31.3° for 3.07mm diameter drops and 8.0m/s and 29.4° for 4.06mm diameter drops, respectively (Fig. 10). Drop stain areas corresponding to impact angles of 31.3° and 29.4° were estimated based on the previous water drop behaviour testing by interpolation between the stain area values corresponding to 25° and 35° angles. To calculate rain amounts for an erosive effect of 5-year time, the areas are multiplied with the approximate monthly average rainfall of 60mm from Lyneham (similar to Boscombe Down), 12 months and 5 years (Fig. 10, Table 4). Using Equation (2) and assuming $\alpha \cdot = 0.222$ and $U = 4.5 m/s$, erosion test water amounts to be released in the form of drops on the surface of bricks was finalised as 400 ml for 3.07mm diameter drops and 900ml for 4.06mm drops (Fig. 10). In different regions with different atmospheric conditions, impacting water amounts and even raindrop size can be determined using region-specific climatic data and on-site measurements ensuring the developed methodology as globally adaptable. Although in reality the spatial and temporal distribution of WDR is discrete and random, for practicality purposes, a uniform flux onto the surface can be assumed.

The bricks were oven dried at a temperature of 110°C for 3 days (mass change was less than 0.1% for a 24 hour interval) and the dry masses measured before erosion testing. Then, they were placed on the angled table and positioned with a digital angle finder (Fig. 11). Two trays were placed at the foot of the bricks to collect the run-off water. After the water impacted on the surface in the form of drops, wet eroded unit masses of the bricks were measured. The bricks were dried in an oven at 110°C for 10 days and then dry eroded unit masses were measured. Material wetting and surface erosion values are calculated according to Equations (6) and (7) and presented in Table 5 and 6. During measurements, material loss by handling the bricks is unlikely as care was taken.

$$Surface\,Erosion = (Dry\,Unit\,Mass - Dry\,Eroded\,Unit\,Mass)/Dry\,Unit\,Mass \times 100\ [\%] \tag{6}$$

$$Wetting = (Wet\,Eroded\,Unit\,Mass - Dry\,Eroded\,Unit\,Mass)/Dry\,Eroded\,Unit\,Mass \times 100\ [\%] \tag{7}$$

### 5.2. Determination of Surface Strength Degradation

The Drilling Resistance Measurement System (DRMS) equipment is used to measure the force required to drill through a solid material and correlate this to the material compressive strength. The standard set-up to test building masonry materials uses a 5mm diameter diamond tipped drill bit with a flat tip. The rotational speed is normally 600rpm and the rate of penetration is 5mm/min. More information on DRMS applications can be found elsewhere [55]. The purpose of using the DRMS machine was to measure the drilling resistance variation between the eroded and uneroded spots on the three solid hand-cut historic clay bricks and three unfired clay bricks (Ecoterre). The testing was performed after the surface erosion test to determine whether water drops on a single spot of masonry would cause a reduction in surface material strength due to their erosive impact.

Because unfired clay bricks have relatively low level of bond strength, the DRMS testing was successfully completed on all of the units. However, during the testing of three solid hand-cut historic clay bricks, DRMS drilling machine refused to drill due to the hard nature of the material and over-resistance of aggregate constituents of the material. As a result, only one of the three units could be tested up to almost 8mm depth. Drilling resistance measurements of unfired clay bricks for three eroded spots were taken from the eroded surface, and measurements for three uneroded spots were mostly taken from the grooves in between the ridges (Fig. 12) for each of the three units. Fig. 13 illustrates the average drilling resistance forces required for the DRMS machine with increasing depth for the unfired clay bricks tested horizontally in the erosion test subjected to both 3.07mm and 4.06mm diameter water drop erosive action. The only results of one of the unfired clay bricks are also included for some comparison in Fig. 13. The solid lines represent the averaged measurements taken from uneroded spots while the dotted lines represent measurements from the eroded spots of each set of three units.

## 6. Results and Discussion

The raindrop impact on masonry materials was examined. To correlate drop behaviour and compare the effects of each parameter, a stain aspect ratio (SAR) has been defined as an indicator of drop behaviour. The ratio provides the normalisation of the measured width and length of drop stain on the surface in a way that the ratio of 1 represents a circular drop stain and the deviation from 1 gives information about the deviation from circular drop stain facilitating the comparison of different size of drops' impact. The SAR, however, does not provide the quantity of water adhering, penetrating or running off, which were recorded with a high speed camera for each drop. SARs of all of the impacting water drops and their associated behaviour on chosen masonry materials were presented in Fig. 5. Each column of SAR represents a single water drop.

### 6.1. The effect of angle and its implications

The general trend of the SAR tends to approach 1 for larger impact angles and 0 for smaller impact angles (Table 7). At 25°, 35° and 45° impact angles, the dominant behaviour is splashing such that 82% of the drops released in all tests splash and 12.5% of drops run off after impingement. At 15° impact angle, the number of splashing drops falls to 67% with a slight increase in bouncing behaviour (17%) and no change in running off drops. However, at a 5° impact angle, the number of splashing drops decreases dramatically to 29% with a dramatic increase in the number of bouncing drops as 63%. Average SAR values increase with impact angle, (Table 7), which actually puts great emphasis on the role of impact angle on the drop behaviour.

This leads to certain deductions. (i) One of the physical implications is that raindrops with high speeds of wind, (impacting under larger angles) tend mostly to splash approaching a SAR of 1 while drops with low wind speeds with smaller angles are more likely to bounce approaching a SAR of 0 (Fig. 5). (ii) Secondly, in terms of the effects on building fabric, splashing causes the masonry unit surfaces to hold a greater amount of water, which could cause water to penetrate into the material more easily, especially for the ones with high porosity. (iii) Thirdly, as Heathcote [11] states, maximum release of kinetic energy takes place at an impact angle of 90°, however, only very strong winds can drive raindrops perpendicular to the vertical wall façades. Drops striking a wall surface at around 45° with SARs close to 1, both transfer most of their kinetic energies onto the wall and erosion takes place due to the resulting prising force [11]. For instance, a drop with a SAR less than 0.3 for the 5° and 15° impact angles are likely to bounce or run off and thus less water is held by the surface. (iv) Additionally, bouncing drops with very low SAR can be caught by WDR gauges and measurements are used in numerical analyses but in reality they would not increase significantly the moisture content of a wall.

### 6.2. The effect of surface roughness, material moisture absorption features and drop velocity

All of the materials are considerably rough since a relatively small roughness of $R_a \approx 0.5\mu m$ can be considered a threshold between smooth and rough surfaces [56]. The influence of roughness is seen in the results. Fired clay bricks (Berkley Red Multi) have the roughest surface among the four tested materials and they cause drops to splash the most except only for the drops with impact angle 5° in Tests 1 and 2. Considerable roughness of lime mortar possibly causes the adhesion of small drops (1.98mm diameter) at modest impact angles. Roughness also plays a role on the splashing behaviour of drops; such that, fingers were generated and their lengths have a profound effect on the variation of the SAR with impact angle. For instance, in Test 4, the stains on fired clay bricks for 25° and 35° deviated slightly from the usual trend because two fingers of the splashing drops were as long as 7mm and 9mm respectively of 2mm width. Similarly, the reason for deviation of the SAR of 4mm diameter drop on lime mortar at 25° impact angle in Test 4 was due to a finger 3mm long and 2mm wide. Given the fact that these two materials have the highest roughness values, surface asperities initiate splashing by disturbing the spreading lamella during drop impact especially the ones with high impact speeds as a generally accepted behaviour on rough surfaces [56]. Additionally, the relative effect of $c_{wi,s}$ and $w_m$ values can not, principally, be observed in the immediate impact behaviour as it takes a few milliseconds to occur superficially. However, absorption features have influence to a certain degree. For instance, relatively high $c_{wi,s}$ and $w_m$ values of lime mortar caused mostly adhesion and splashing. Possibly, due to the closeness of impact speeds of the same size of drops, their impact behaviour does not present quite noticeable difference.

### 6.3. The effect of drop size

As the drop size increases, water drops tend to splash and run-off more. For example, at a 15° impact angle, 4.06mm drops splash; while 1.95mm and 3.07mm diameter drops bounce on solid hand-cut historic bricks. From the erosivity point of view, more kinetic energy of drops are released during adherence and splashing then bouncing because when a drop bounces it keeps some of its kinetic energy after hitting the surface by continuing its move with a velocity. Therefore, bigger size drops at higher impact angles will transfer more energy on the facades by adhering, which could cause relatively more erosion over time. Furthermore, larger drops apply larger pressures on the surface. To understand the impact forces, Nearing et. al. [57] measured force and time relationships of water drop impact. They released drops with diameters of 3.31mm, 3.83mm, 4.51mm, and 5.25mm from a height of 14.0m onto piezoelectric transducers with rise times of 2 and 5μs. They calculated average water drop impact pressures using the force measurements and an approximation of water drop contact area as a function of time. Results show that larger drops do not necessarily suggest greater impact pressures however they certainly indicate that greater pressures are produced for longer durations. Therefore larger drops are critical for exposure of surfaces. Average pressures decrease to 100kPa after 50μs. The maximum average pressure for the 5.25mm diameter drop was found as high and powerful as 1.3MPa [57]. This repetitive and long-term impact pressure becomes critical when compressive strength of unfired clay bricks (Ecoterre) as 3.8MPa and fired clay bricks (Berkeley Red Multi) as about 40MPa are taken into account. Shear strength values of these materials are even less.

### 6.4. Surface erosion

Permanent actions of these pressures induced by WDR drops render material erosion. For the relative quantification of erosion, and wetting, three solid hand-cut historic clay bricks and three unfired clay bricks (Ecoterre) were tested (Table 5 and 6). An impact angle of 30º is considered to be an optimum value for erosion tests based on wind and drop terminal velocity analysis (Fig. 10) being comparable with the values used in similar tests [53]. Considering impact behaviour tests, at a 30º impact angle, splashing is expected for all of the drop behaviour except for the 4.06mm diameter drops, running off after impacting on unfired clay bricks. This will ensure maximum kinetic energy release during impingement.

It is experimentally verified that rain water drop impact causes surface erosion. Table 5 presents the results of Solid hand-cut historic clay brick erosion test (Test 1). Because the bond strength of the particles of the solid hand-cut historic clay bricks is very strong, very slight erosion has been observed. Hence, no substantial difference was identified in terms of drop size in surface erosion. The very slight variation of surface erosion between brick units might be due to the heterogeneity of the brick fabric and the varying strength characteristics of the units gained mainly during the firing process. However, the wetting impact of the water drops was profound. Agreeably wetting values of the brick units confirm the effect of high $c_{wi,s}$ and $w_m$ values for Solid hand-cut fired bricks (Table 3 and 5). As high as 10.4% wetting was observed during the erosion test of 4.06mm drops. The clear implication of this is the important role of water drop impact on the masonry wall wetting.

The results of the unfired clay bricks (Ecoterre) in Erosion Test 2 show that surface erosion values fluctuate around 1% for both 3.07 mm and 4.06mm diameter drops, representing material loss (Table 6). However a slightly less erosion (0.19%) is observed for the 4.06 mm diameter drops. This is attributed to the fact that the impact pressures of the 4.06 mm diameter drops were higher than the 3.07mm diameter drops [57]. This erosive effect caused pitting on the surface and the pits acted as a drainage after a while directing water down into the run-off water collection trays. That is, gradual erosion of the ridges of the horizontally laid bricks created vertical grooves and allowed the water to run off. Moreover, impact behaviour tests agreeably imply that drops on unfired clay bricks at a 30° impact angle run off. Comparison of the wetting of the tested materials shows that the unfired clay bricks had lower wetting values. In conclusion, the solid hand-cut clay bricks have a higher permeability and hence retain more water as opposed to the low permeability of the unfired clay bricks that prevented more water from being absorbed into the brick. The long-term effect of moisture embodied by WDR, especially over variable temperature spells, can be deterioration. The erosion test proposed critical and globally practical results for the assessment of different masonry materials.

The eroded areas were not very visible on solid hand-cut historic clay bricks. However, material detachment was quite evident on unfired clay bricks since the erosion process started when the surface became wet enough to revert back to loose clay and erode until the aggregates had been reached. Then, the rate of erosion slowed down considerably. The fact that the resulting loose surface fabric may reduce the material surface strength increased the considerations of testing strength variation through eroded and uneroded areas after erosion tests. As a result, both materials were tested using DRMS.

### 6.5. Surface strength reduction due to drop impact

The resistance of masonry units to drilling in terms of force thorough their depth are shown in Fig. 13. They generally show that for up to a depth of about 8 mm, the eroded spots show strikingly a lower drilling resistance than the uneroded spots. Even though the eroded spots are at a lower datum (aggregates present at the surface) than the uneroded spots, they consistently exhibit a lower drilling resistance at the start of the measurement due to strength degradation throughout the layers near surface. Within the first 3mm from the surface more than 40% strength seems to be lost. Furthermore, stronger drop impact rendered greater strength degradation. Slightly lower strength resistance of eroded spots by 4.06mm diameter drops than by 3.07mm diameter drops is evident in Fig. 13. This indicates that larger drops have larger impacts on the surface degradation applying larger forces for longer durations. Measurements taken from uneroded spots agree quite well, demonstrating the testing reliability. From the surface to a point of 8mm depth, material resistance increases significantly due to the substance graining and resultant weakened bond strength of material near surface. After that point, however, resistance to drilling follows a very slightly increasing trend due to the side friction of the probe. In addition, no strength degradation due to the water drop impact is observed and resistance at the eroded and uneroded spots behave similar throughout the rest of the depth (Fig. 13).

Comparison of the testing results of hand-cut historic clay bricks and unfired clay brick (Ecoterre) shows that if the material bond strength is higher, the surface strength reduction decreases and consequently less erosion takes place. For example, within the first 3mm from the surface while the water drop impact causes considerable and consistent strength reduction on unfired clay bricks (Ecoterre), a slight and varying reduction is seen on solid hand-cut historic clay bricks. Furthermore, the fact that fired bricks show 2.3 times more resistance than the unfired ones at the point of 7mm deep proves evident.

## 7. Conclusions

Widespread and severe recent flood events have raised concerns about the increase in rainfall intensities. Winters and autumns have become wetter relative to previous decades. The increase in rainfall and changes in wind speed patterns have serious implications on the surface erosion of cultural heritage. Particle detachment occurs through long-term, continuous, repetitive and synergetic action of WDR. The major factors of gradual surface erosion can be classified into four components of loss: values, hazard, vulnerability and exposure in predictions. Firstly, a parametric WDR impact behaviour testing was performed where solid hand-cut historic clay bricks, fired clay bricks (Berkeley Red Multi), unfired clay bricks (Ecoterre), and lime mortar with various vulnerabilities were tested in order to better understand masonry material response to varying hazard intensities employing three drop diameters, six impact speeds and five impact angles. The behaviour is quite complicated for exact correlation. Therefore a stain aspect ratio (SAR) is defined as the ratio of drop stain width to stain length. SAR tends to approach to 1 for larger impact angles (strong winds) denoting splashing drops and to 0 denoting bouncing drops. It gives information about the erosive effect of a drop in terms of energy release, wall surface wetting effect and potential error for WDR measurements. It was seen that the behaviour of drops changes depending on the drop characteristics and masonry material. The rougher the surface, the more splashing occurred and even fingering was observed. Additionally, as the drop size gets bigger, water drops tend to do more splashing and run-off after striking the surface. Then, a straightforward and globally adaptable testing method has been introduced for an erosion weatherability assessment to evaluate the performance of three solid hand-cut historic clay bricks and three unfired clay bricks (Ecoterre) for two impacting drop sizes. Surface erosion and resulting wetting were quantified. Unfired clay bricks showed relatively much higher erosion owing to their low bond strength and solid hand-cut historic clay bricks were wetted more due to their high permeability. The drilling resistance measurement system equipment is used to measure the strength variation through the eroded and uneroded spots on masonry units after erosion tests. For up to a depth of about 8 mm, the eroded spots showed a lower drilling resistance than the uneroded spots for unfired clay bricks. While the above work experimentally validates and attempts to quantify the extent of surface erosion and material strength degradation as a function of rain and material properties, it is necessary to apply this approach to a larger variety of masonry materials to be more confident in predictions and develop preventive measures for sustainability of cultural heritage.

**Acknowledgements**

The authors greatly acknowledge the assistance of Dr. Michael Lawrence and the technicians William Bazeley and Sophie Hayward in the Structures Laboratories of the University of Bath, UK.

**References**

[1] The Met Office, the UK's National Weather Service. Web site: http://www.metoffice.gov.uk/weather/uk/; Accessed on February 1, 2010.
[2] Drdacky M. Binda L. Hennen IC. Kopp C. Lanza L.G. Helmerich R. Cultural heritage protection against flooding. Prague: Institute of Theoretical and Applied Mechanics AS CR; 2011.
[3] Bonazza A, Messina P, Sabbioni C, Grossi CM, Brimblecombe P. Mapping the impact of climate change on surface recession of carbonate buildings in Europe. Sci Total Environ 2009; 407: 2039-2050.
[4] Amoroso GG, Fassina V. Stone decay and conservation: atmospheric pollution, cleaning, consolidation and protection. Materials Science Monographs, 11, Elsevier Science Publishers, Amsterdam; 1983.
[5] Livingston RA. Graphical methods for examining the effects of acid rain and sulfur dioxide on carbonate stones. Proceedings of the Seventh International Congress on Deterioration and Conservation of Stone, Lisbon, Portugal; June 15-18, 1992.
[6] Tang W, Davidson CI, Finger S, Vance K. Erosion of limestone building surfaces caused by wind-driven rain: 1. field measurements. Atmos Environ 2004; 38: 5589-5599.
[7] Tang W, Davidson CI. Erosion of limestone building surfaces caused by wind-driven rain: 2. numerical modelling. Atmos Environ 2004; 38: 5601-5609.
[8] Etyemezian V, Davidson CI, Zufall M, Dai W, Finger S, Striegel M. Impingement of rain drops on a tall building. Atmos Environ 2000; 34: 2399-2412.
[9] Briggen PM, Blocken B, Schellen HL. Wind-driven rain on the facade of a monumental tower: numerical simulation, full-scale validation and sensitivity analysis. Build Environ 2009; 44: 1675-1690.
[10] Young ME. Dampness penetration problems in granite buildings in Aberdeen, UK: causes and remedies. Constr Build Mater 2007; 21: 1846-1859.
[11] Heathcote KA. Durability of earthwall buildings. Constr Build Mater 1995; 9: 185-189.
[12] Jayasinghe C, Kamaladasa N. Compressive strength characteristics of cement stabilized rammed earth walls. Constr Build Mater 2007; 21: 1971-1976.
[13] Kerali AG. Durability of compressed and cement-stabilised building blocks. PHD Thesis, University of Warwick, 2001.
[14] Blocken B, Carmeliet J. A review of wind-driven rain research in building science. J Wind Eng Ind Aerod 2004; 92: 1079-1130.
[15] Kron W. Flood Risk = Hazard • Values • Vulnerability. Water Int 2005; 30: 58–68.
[16] McCullagh RPJ. Excavations at Sueno's Stone, Forres, Moray. Proc Soc Antiq Scot 1995; 125: 697-718.
[17] Caroe MB. Wells Cathedral conservation of figure sculptures, 1975-1984. Bulletin of the Association for Preservation Technology, APT 1985; 17: 2-13.
[18] Murphy JM, Sexton DMH, Jenkins GJ, Boorman PM, Booth BBB, Brown CC, et al. UK climate projections science report: climate change projections, Met Office Hadley Centre, Exeter; 2009.
[19] Smith BJ, McCabe S, McAllister D, Adamson C, Viles HA, Curran JM. A commentary on climate change, stone decay dynamics and the 'greening' of natural stone buildings: new perspectives on 'deep wetting. Environ Earth Sci 2010; 63: 1691-1700.

[20] Jenkins GJ, Perry MC, Prior MJ. The climate of the United Kingdom and recent trends. Met Office Hadley Centre, Exeter, UK; 2008.

[21] Lacy RE. Climate and building in Britain. London: Her Majesty's Stationery Office; 1977.

[22] Blocken B, Carmeliet J. Overview of three state-of-the-art wind-driven rain assessment models and comparison based on model theory. Build Environ 2010; 45: 691-703.

[23] ISO. Hygrothermal performance of buildings – Calculation and presentation of climatic data – Part 3: Calculation of a driving rain index for vertical surfaces from hourly wind and rain data. ISO 15927-3:2009 International Organization for Standardization; 2009.

[24] Yarin AL. Drop impact dynamics: splashing, spreading receding, bouncing…. Annu Rev Fluid Mech 2006; 38: 159-192.

[25] Fedorchenko, AI, Wang AB. On some common features of drop impact on liquid surfaces. Phys Fluids 2004; 16: 1349-1365.

[26] Rioboo R, Marengo M, Tropea C. Time evolution of liquid drop impact onto solid, dry surfaces. Exp Fluids 2002; 33: 112-124.

[27] Eggers J, Fontelos MA, Josserand C, Zaleski S. Drop dynamics after impact on a solid wall: theory and simulations. Phys Fluids 2010; 22: 062101-062101.

[28] Chen PP, Wang XS. Experimental study of water drop impact on wood surfaces. Int J Heat Mass Tran 2011; 54: 4143-4147.

[29] Gu Y, Li D. Liquid drop spreading on solid surfaces at low impact speeds. Colloid Surface A 2000; 163: 239-245.

[30] Adler WF. Waterdrop impact modeling. Wear 1995; 186-187: 341-351.

[31] Abuku M, Blocken B, Poesen J, Roels S. Spreading, splashing and bouncing of wind-driven raindrops on building facades, 11th Americas Conference on Wind Engineering, San Juan, Puerto Rico; June 22-26, 2009.

[32] Chandra S.; Avedisian CT. Observations of droplet impingement on a ceramic porous surface. Int J Heat Mass Tran 1992; 35: 2377-2388.

[33] Zadrazil A, Stepanek F, Matar OK. Droplet spreading, imbibition and solidification on porous media. J Fluid Mech 2006; 562: 1-33.

[34] Rioboo R, Tropea C, Marengo M. Outcomes from a drop impact on solid surfaces. Atomization Spray 2001; 11: 151–165.

[35] Abuku M, Janssen H, Poesen J, Roels S. Impact, absorption and evaporation of raindrops on building facades. Build Environ 2009; 44: 113-124.

[36] Choi ECC. Wind-driven rain and driving rain coefficient during thunderstorms and non-thunderstorms. J Wind Eng Ind Aerod 2001; 89: 293-308.

[37] Fernández-Raga M, Castro A, Palencia C, Calvo AI, Fraile R. Rain events on 22 October 2006 in León (Spain): Drop size spectra. Atmos Res 2009; 93: 619-635.

[38] Jayawardena AW, Rezaur RB. Measuring drop size distribution and kinetic energy of rainfall using a force transducer, Hydrol Process 2000; 14: 37-49.

[39] Szakáll M, Mitra SK, Diehl K, Borrmann S. Shapes and oscillations of falling raindrops — a review. Atmos Res 2010; 97: 416-425.

[40] Best AC. The size distribution of raindrops. Q J Roy Meteor Soc 1950; 76: 16-36.

[41] Blocken B, Carmeliet J. Driving rain on building envelopes- I. numerical estimation and full-scale experimental verification. J Build Phys 2000; 24: 61-85.

[42] Oti JE, Kinuthia JM, Bai J. Engineering properties of unfired clay masonry bricks. Eng Geol 2009; 107: 130-139.

[43] Blocken B, Abuku M, Roels S, Carmeliet J. Wind-driven rain on building facades: some perspectives, EACWE 5 Florence, Italy; July 19-23, 2009.

[44] Wenzel RN. Resistance of solid surfaces to wetting by water, Ind Eng Chem 1936; 28: 988–995.

[45] Cassie ABD, Baxter S. Wettability on porous surfaces, Trans Faraday Soc 1944; 40: 546–549.

[46] Vaikuntanathan V, Kannan R, Sivakumar D. Impact of water drops onto the junction of a hydrophobic texture and a hydrophilic smooth surface. Colloid Surface A 2010; 369: 65-74.

[47] Gipperich A, Lembach AN, Roisman IV, Tropea C. On the splashing threshold of a single droplet impacting onto rough and porous surfaces. Proc ILASS Europe 2010 Brno, Czech Republic.

[48] Marengo M, Antonini C, Roisman IV, Tropea C. Drop collisions with simple and complex surfaces. Curr Opin Colloid In 2011; 16: 292-302.

[49] BS EN ISO 4287:1998+A1:2009 Geometrical product specification (GPS). Surface texture: Profile method. Terms, definitions and surface texture parameters.

[50] BS EN 772-11:2000, British Standard, Methods of test for masonry units, Part 11.

[51] Hall C. Water movement in porous building materials-IV. The initial surface absorption and the sorptivity. Build Environ 1981; 16: 201-207.

[52] BS EN 771-1:2003, British Standard, Specification for masonry units, Part 1: Clay Masonry Units.

[53] Heathcote KA. An investigation into the erodibility of earth wall units. PhD Thesis, University of Technology, Sydney: 2002.

[54] Salles C, Poesen J. Rain properties controlling soil splash detachment. Hydrol Process 2000; 14: 271-282.

[55] Lawrence RMH, Walker P. The measurement of the carbonation profile in lime mortars using a drilling resistance measurement system. Proceedings of the 11th International Congress on Deterioration and Conservation of Stone, Torun, Poland, September 15-20, 2008. pp.415-423.

[56] Rein M, Delplanque JP. The role of air entrainment on the outcome of drop impact on a solid surface. Acta Mech 2008; 201: 105-118.

[57] Nearing MA, Bradford JM, Holtz RD. Measurement of force vs. time relations for waterdrop impact. Soil Sci Soc Am J 1986; 50: 1532-1536.


**Figure Captions**

**Fig. 1.** Various locations on SE and SW façades of the southern transept of Tewkesbury Abbey
**Fig. 2.** Seasonal rainfall variation in the UK
**Fig. 3.** Schematic illustration of testing set-up
**Fig. 4.** Impact behaviour of the 4.06mm diameter droplet from a height of 4.0m on the solid hand-cut historic clay brick at 5°
**Fig. 5.** Stain aspect ratios of water drops on masonry material with respect to impact angle
**Fig. 6.** Water drop stains on the tested masonry materials after impact
**Fig. 7.** Laser scanning for surface roughness determination and resultant roughness profile of solid hand-cut historic clay brick
**Fig. 8.** Initial rate of water absorption testing of solid hand-cut historic clay bricks
**Fig. 9.** Monthly rainfall and wind speed averages in Boscombe Down and Lyneham between 1971 and 2000
**Fig. 10.** Rain intensity vectors (RIV) and water volume representation for erosion test
**Fig. 11.** Brick units on angled table during erosion test
**Fig. 12.** Testing strength variation of eroded unfired clay brick (Ecoterre) by DRMS machine through the depth of the units
**Fig. 13.** Averaged DRMS data from eroded and uneroded spots of unfired clay bricks (Ecoterre) tested with 3.07mm and 4.06mm diameter drops and DRMS data from eroded and uneroded spots of solid hand-cut historic clay brick tested with 3.07mm □ drops (only one tested unit results)

**Table Captions**

Table 1 Water drop behaviour tests combination.
Table 2 Surface roughness of tested materials.
Table 3 Absorption test results of the materials.
Table 4 Interpolated stain areas.
Table 5 Erosion Test 1 – Solid hand-cut historic clay brick erosion test results.
Table 6 Erosion Test 2 – Unfired clay bricks (Ecoterre) erosion test results.
Table 7 Number of drops in the impact behaviour tests.

Table1 Water drop behaviour tests combination.

| Parameters | Test 1 | Test 2 | Test 3 | Test 4 | Test 5 | Test 6 |
|---|---|---|---|---|---|---|
| Drop Diameter (mm) | 1.95 | 3.07 | 3.07 | 4.06 | 4.06 | 4.06 |
| Falling Height (m) | 2.10 | 2.10 | 3.20 | 2.10 | 3.20 | 4.00 |
| Drop Speed (m/s) | 5.75 | 6.00 | 6.92 | 6.06 | 7.29 | 8.00 |

Table 2 Surface roughness of tested materials.

| Masonry Type | Direction | Roughness (μm) | | | | | | | |
|---|---|---|---|---|---|---|---|---|---|
| | | Test 1 | Test 2 | Test 3 | Test 4 | Test 5 | Direction Average | Standard Deviation | Final Average |
| Solid hand-cut historic clay brick (Victorian) | x | 58.30 | 48.40 | 46.40 | 47.50 | 56.00 | 51.32 | 5.43 | 50.37 |
| | y | 48.60 | 54.20 | 45.80 | 50.60 | 47.90 | 49.42 | 3.18 | |
| Fired clay brick (Berkeley Red Multi) | x | 272.70 | 131.40 | 280.10 | 198.80 | 335.10 | 243.62 | 79.29 | 231.88 |
| | y | 173.70 | 200.70 | 139.70 | 316.30 | 270.30 | 220.14 | 72.06 | |
| Unfired clay bricks (Ecoterre) | x | 32.50 | 29.90 | 31.50 | 28.50 | 32.40 | 30.96 | 1.73 | 13 |
| | y | 12.40 | 14.40 | 12.20 | 12.40 | 13.60 | 13.00 | 0.96 | |
| Lime Mortar | x | 105.60 | 105.90 | 43.10 | 70.00 | 45.10 | 73.94 | 30.91 | 76.62 |
| | y | 106.40 | 89.00 | 49.70 | 86.10 | 65.30 | 79.30 | 22.06 | |

Table 3 Absorption test results of the materials.

| **Material** | $C_{wi,s}$ $[kg/(m^2 \times \min)]$ | $w_m$ [%] |
|---|---|---|
| Solid hand-cut historic clay bricks | 1907.2 | 12.71 |
| Fired clay bricks (Berkeley Red Multi) | 505.1 | 4.56 |
| Lime mortar | 1109.6 | 19.95 |

Table 4 Interpolated stain areas.

| Drop Diameter (mm) | Fired clay bricks (Berkeley Red Multi) | | Unfired clay bricks (Ecoterre) | |
|---|---|---|---|---|
| | Stain area ($cm^2$) | 5 year volume ($cm^3$) | Stain area ($cm^2$) | 5 year volume ($cm^3$) |
| 3.07 | 1.142 | 411.12 | 1.11 | 399.6 |
| 4.06 | 2.50 | 900 | 3.04 | 1094.4 |

Table 5 Erosion Test 1 – Solid hand-cut historic clay brick erosion test results

| Drop Diameter (mm) | Unit No | Dry Unit Mass (grams) | Wet Eroded Unit Mass (grams) | Dry Eroded Unit Mass (grams) | Wetting (%) | | | Surface Erosion (%) | | |
|---|---|---|---|---|---|---|---|---|---|---|
| | | | | | $x$ | $\bar{x}$ | $\sigma$ | $x$ | $\bar{x}$ | $\sigma$ |
| 3.07 | 1 | 2937.8 | 3196.5 | 2937.6 | 8.81 | 9.17 | 0.33 | 0.0068 | 0.0145 | 0.011 |
| | 2 | 3063.8 | 3346.8 | 3063.5 | 9.25 | | | 0.0098 | | |
| | 3 | 2957.7 | 3236.4 | 2956.9 | 9.45 | | | 0.0270 | | |
| 4.06 | 4 | 3003.5 | 3316.5 | 3003.4 | 10.42 | 8.90 | 1.40 | 0.0033 | 0.0086 | 0.005 |
| | 5 | 3075.3 | 3310.9 | 3074.9 | 7.68 | | | 0.0130 | | |
| | 6 | 3164.7 | 3436.2 | 3164.4 | 8.59 | | | 0.0095 | | |

Table 6 Erosion Test 2 – Unfired clay bricks (Ecoterre) erosion test results

| Drop Diameter (mm) | Unit No | Dry Unit Mass (grams) | Wet Eroded Unit Mass (grams) | Dry Eroded Unit Mass (grams) | Wetting (%) | | | Surface Erosion (%) | | |
|---|---|---|---|---|---|---|---|---|---|---|
| | | | | | $x$ | $\bar{x}$ | $\sigma$ | $x$ | $\bar{x}$ | $\sigma$ |
| 3.07 | 1 | 3114.6 | 3158.5 | 3081.6 | 2.50 | 3.24 | 0.66 | 1.0595 | 1.0230 | 0.102 |
| | 2 | 3115.9 | 3194.6 | 3087.6 | 3.47 | | | 0.9082 | | |
| | 3 | 3105.4 | 3186.6 | 3071.2 | 3.76 | | | 1.1012 | | |
| 4.06 | 4 | 3123.5 | 3181.8 | 3096.6 | 2.75 | 3.49 | 0.69 | 0.8612 | 0.8293 | 0.061 |
| | 5 | 3111.9 | 3195.9 | 3084.9 | 3.60 | | | 0.8676 | | |
| | 6 | 3148.3 | 3253.2 | 3124.4 | 4.12 | | | 0.7591 | | |

Table 7 Number of drops in the impact behaviour tests.

| Units | Impact Behaviour | Impact Angle | | | | |
|---|---|---|---|---|---|---|
| | | 5° | 15° | 25° | 35° | 45° |
| Solid hand-cut historic clay bricks | Bouncing | 5 | 3 | 1 | 1 | 0 |
| | Running-off | 0 | 0 | 0 | 0 | 0 |
| | Adhesion | 0 | 0 | 0 | 0 | 0 |
| | Splashing | 1 | 3 | 5 | 5 | 6 |
| | Average SAR | 0.04 | 0.21 | 0.37 | 0.53 | 0.76 |
| Fired clay bricks (Berkeley Red Multi) | Bouncing | 2 | 0 | 0 | 0 | 0 |
| | Running-off | 0 | 0 | 0 | 0 | 0 |
| | Adhesion | 0 | 0 | 0 | 0 | 0 |
| | Splashing | 4 | 6 | 6 | 6 | 6 |
| | Average SAR | 0.07 | 0.25 | 0.42 | 0.59 | 0.66 |
| Unfired clay bricks (Ecoterre) | Bouncing | 4 | 1 | 0 | 0 | 0 |
| | Running-off | 2 | 3 | 3 | 3 | 3 |
| | Adhesion | 0 | 0 | 0 | 0 | 0 |
| | Splashing | 0 | 2 | 3 | 3 | 3 |
| | Average SAR | 0.09 | 0.22 | 0.39 | 0.53 | 0.72 |
| Lime mortar | Bouncing | 4 | 0 | 0 | 0 | 0 |
| | Running-off | 0 | 0 | 0 | 0 | 0 |
| | Adhesion | 0 | 1 | 1 | 1 | 0 |
| | Splashing | 2 | 5 | 5 | 5 | 6 |
| | Average SAR | 0.09 | 0.25 | 0.44 | 0.58 | 0.66 |
| Total of the 4 type of units | Bouncing | 15 | 4 | 1 | 1 | 0 |
| | Running-off | 2 | 3 | 3 | 3 | 3 |
| | Adhesion | 0 | 1 | 1 | 1 | 0 |
| | Splashing | 7 | 16 | 19 | 19 | 21 |
| | Average SAR | 0.07 | 0.23 | 0.40 | 0.56 | 0.70 |

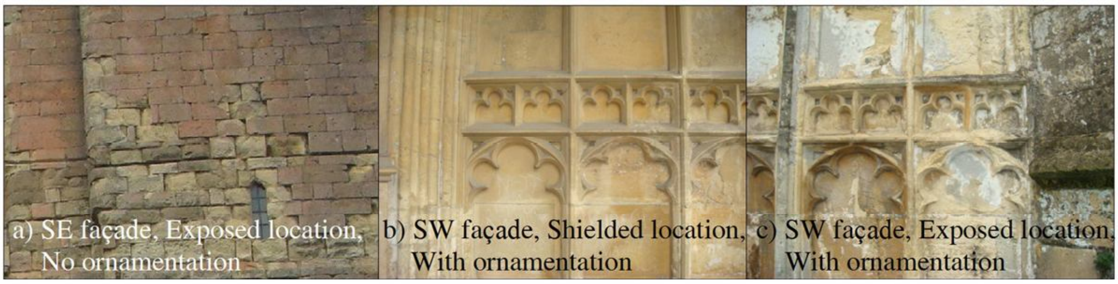
a) SE façade, Exposed location,
No ornamentation
b) SW façade, Shielded location,
With ornamentation
c) SW façade, Exposed location,
With ornamentation

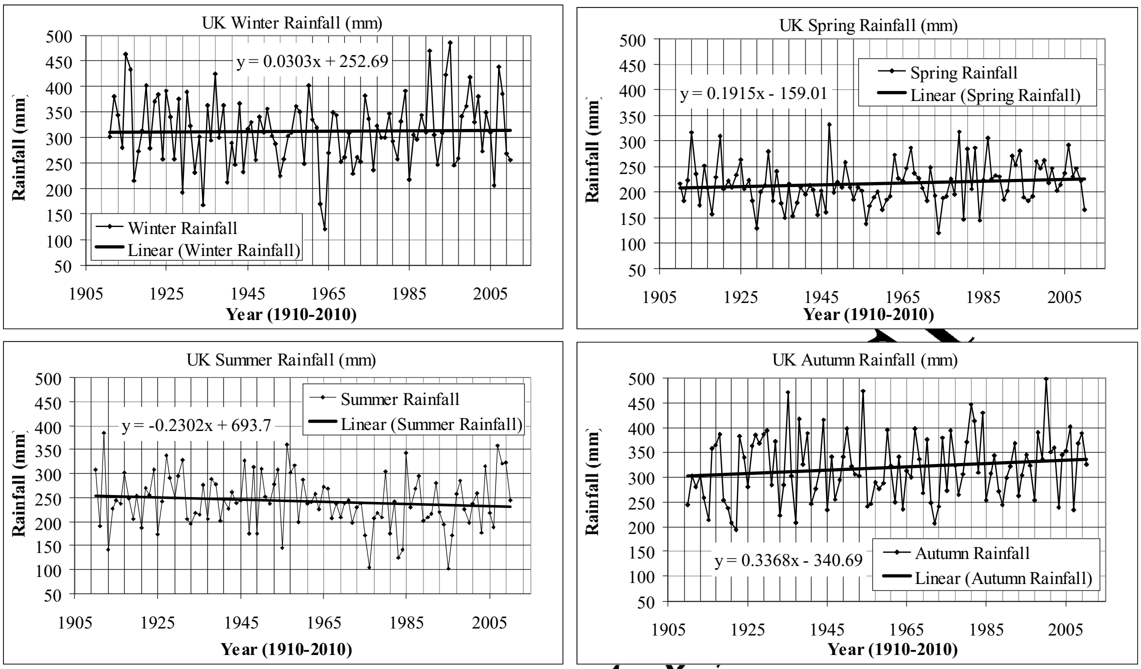


**Fig. 2.** Seasonal rainfall variation in the UK

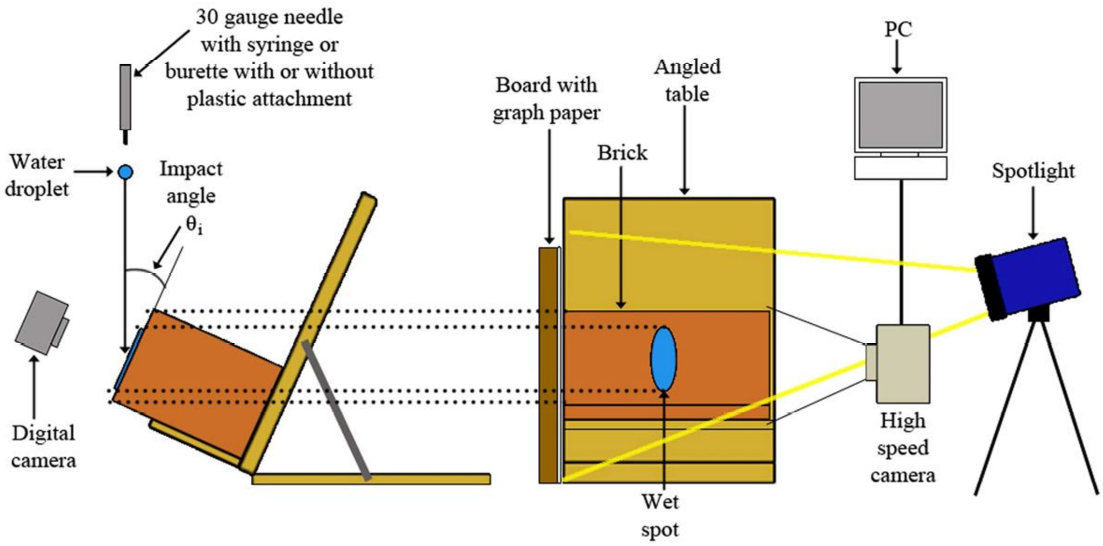
30 gauge needle
with syringe or
burette with or without
plastic attachment
Water
droplet
Impact
angle
$\theta_i$
Digital
camera
Board with
graph paper
Angled
table
Brick
Wet
spot
PC
Spotlight
High
speed
camera

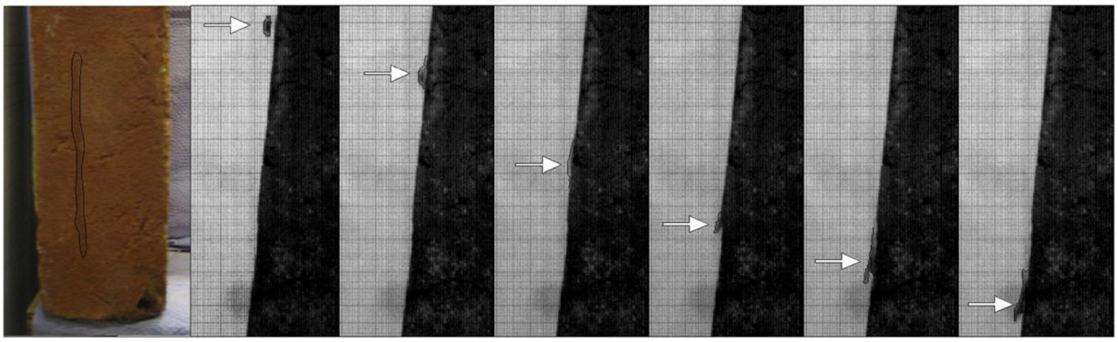

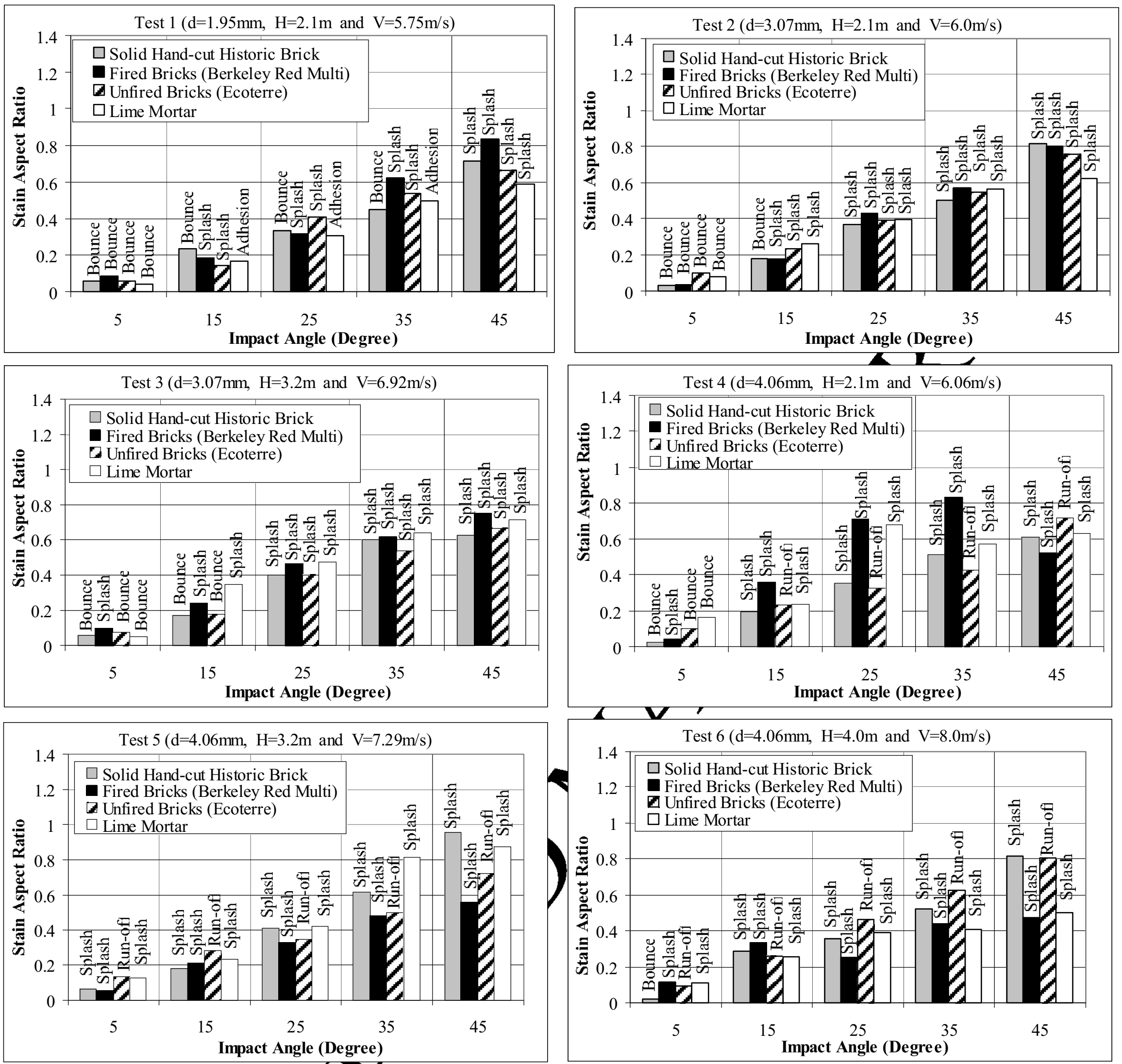


**Fig. 5.** Stain aspect ratios of water drops on masonry material with respect to impact angle

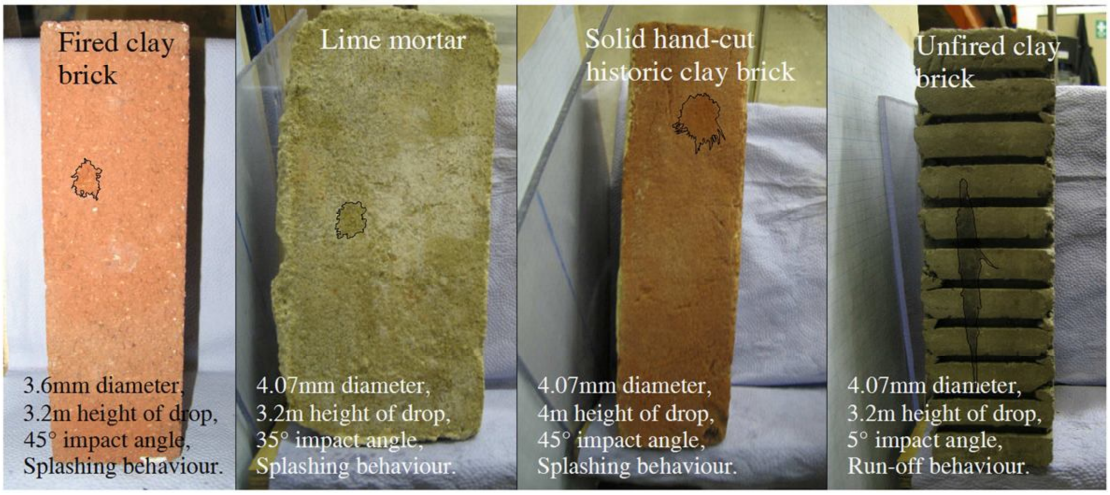
Fired clay brick
3.6mm diameter, 3.2m height of drop, 45° impact angle, Splashing behaviour.
Lime mortar
4.07mm diameter, 3.2m height of drop, 35° impact angle, Splashing behaviour.
Solid hand-cut historic clay brick
4.07mm diameter, 4m height of drop, 45° impact angle, Splashing behaviour.
Unfired clay brick
4.07mm diameter, 3.2m height of drop, 5° impact angle, Run-off behaviour.

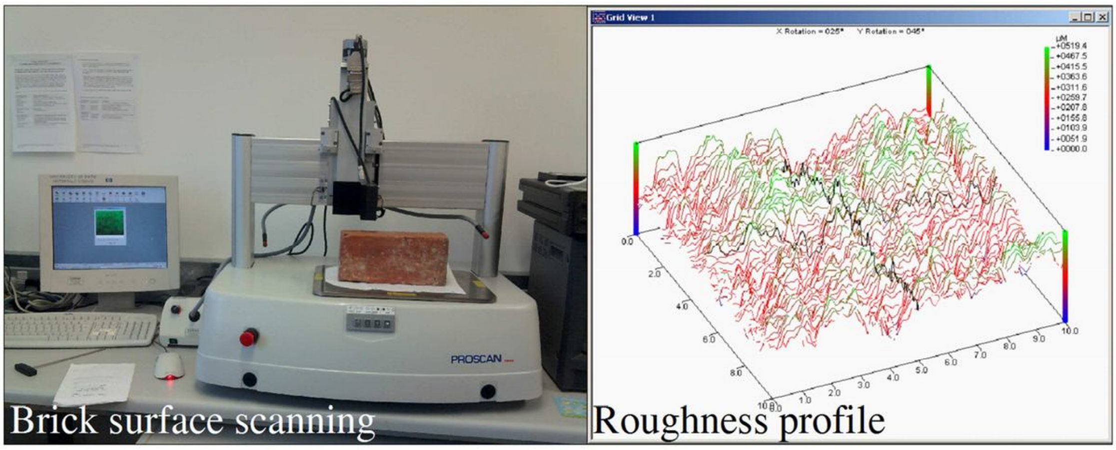
Brick surface scanning
PROSCAN
Roughness profile
Grid View 1

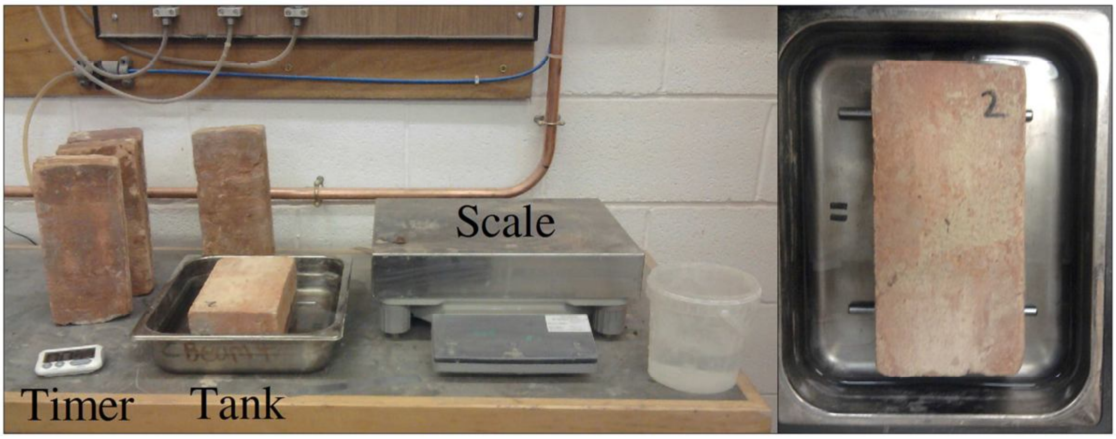
Scale
Timer
Tank
2

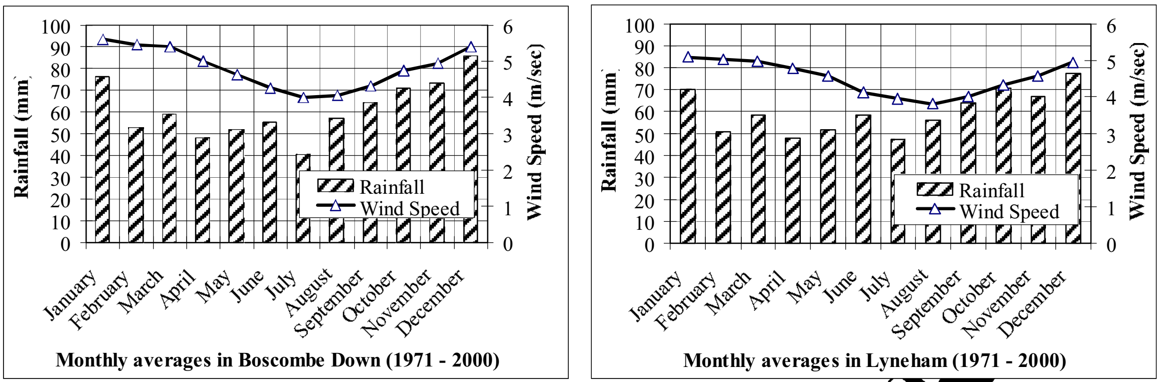


**Fig. 9.** Monthly rainfall and wind speed averages in Boscombe Down and Lyneham between 1971 and 2000

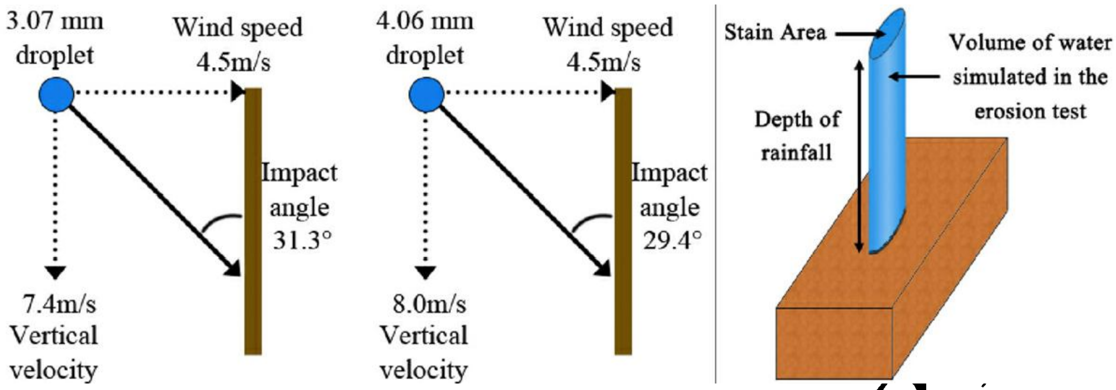
3.07 mm
droplet
Wind speed
4.5m/s
Impact
angle
31.3°
7.4m/s
Vertical
velocity
4.06 mm
droplet
Wind speed
4.5m/s
Impact
angle
29.4°
8.0m/s
Vertical
velocity
Stain Area
Volume of water
simulated in the
erosion test
Depth of
rainfall


Solid hand-cut historic bricks
Unfired clay bricks

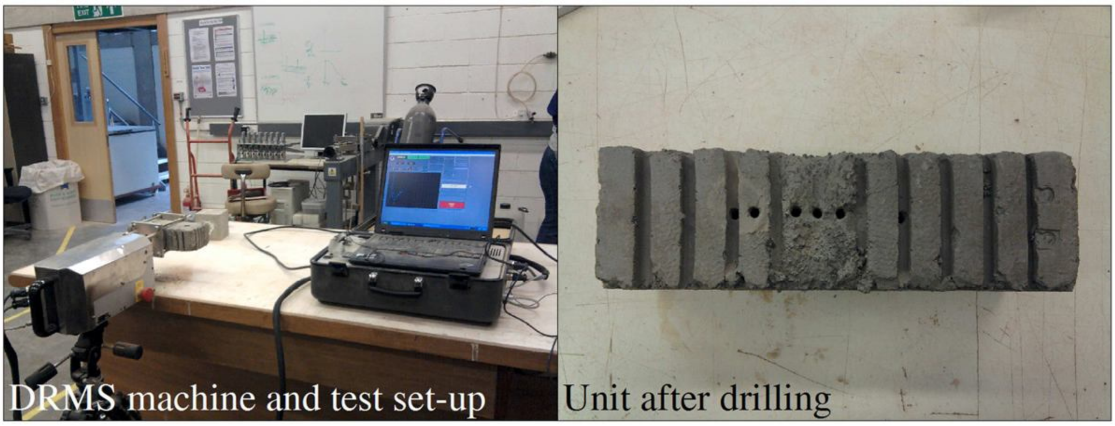
DRMS machine and test set-up
Unit after drilling

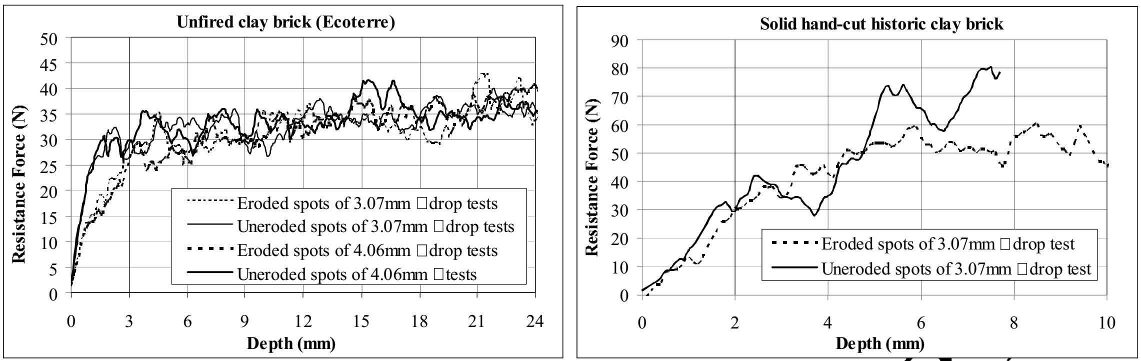


**Fig. 13.** Averaged DRMS data from eroded and uneroded spots of unfired clay bricks (Ecoterre) tested with 3.07mm and 4.06mm diameter drops and DRMS data from eroded and uneroded spots of solid hand-cut historic clay brick tested with 3.07mm Ø drops (only one tested unit results)

**Highlights**

- Raindrop erosion considering hazard, vulnerability exposure and values is defined
- Physical raindrop impact on masonry surface erosion is comprehensively documented
- Impact angle, drop size, surface roughness are crucial factors in surface response
- Bond strength in erosion and moisture absorption features in wetting are central
- Raindrop induced surface erosion causes strength degradation of building materials